Electronic Supplementary Material (ESI) for Inorganic Chemistry Frontiers.

Supporting Information

Fabrication of amorphous metal oxide/p-$BiVO_4$ photocathode: understanding the role of entropy for reducing nitrate to ammonia

Fengfeng Wang [a], Qijia Ding [a], Yajie Bai [a], Hongye Bai [a]*, Song Wang [b]*, Weiqiang Fan [a]*

[a] *School of Chemistry and Chemical Engineering, Jiangsu University, Zhenjiang, 212013, P. R. China.*

[b] *Hubei Key Laboratory of Low Dimensional Optoelectronic Materials and Devices, Hubei University of Arts and Science, Xiangyang, 441053, PR China.*

E-mail: bhy198412@163.com; wangsong1984@126.com; fwq4993329@yahoo.com

Experimental sections

The synthesis of materials

Chemicals and reagents: Chemicals and reagents were purchased from Sino pharm Chemical Reagent Co., Ltd., and all of them were analytical grade and used without further purification. Deionized water was used in all experiments. Fluorine-doped tin oxide (FTO) glass substrates were ultrasonically pretreated in acetone, ethanol and water, respectively.

Synthesis of p-$BiVO_4$: 0.4851 g $Bi(NO_3)_3 \cdot 5H_2O$ and 0.3722 g EDTA-2Na were dissolved in 10 mL HNO_3 (2 mol L^{-1}) solution. 0.1170 g NH_4VO_3 and 0.3722 g EDTA-2Na were dissolved in 20 mL NaOH (1 mol L^{-1}) solution. Two above solutions were transferred into a Teflon-lined stainless-steel autoclave together with FTO. The autoclave was kept at 160 ℃ for 12 hours, and p-$BiVO_4$ sample was rinsed with deionized water three times and dried at room temperature.

Synthesis of A-M_xO_y/$BiVO_4$: Metal salts of $X(OAc)_2$, YCl_2 (X = Co, Mn and Ni, Y = Fe and Cu) (the specific weight is listed in Table S2) and 0.3 g sodium acetate were mixed with 30 mL ethylene glycol. Then, the mixture was transferred into a Teflon-lined stainless-steel autoclave with p-$BiVO_4$, and kept at 180 ℃ for 1 hour. Afterwards, the autoclave was naturally cooled to room temperature, and the obtained sample was washed with C_2H_5OH for three times and dried in a vacuum oven for 12 hours at 60 ℃.

Characterizations

The crystal structures of samples were analyzed with a Brooke D8 advanced X-ray diffraction (XRD). The morphologies were characterized by a field emission scanning electronic microscopy (FESEM, 3 kV), transmission electron microscopy (TEM) and high resolution TEM (HRTEM，200 kV) coupled with energy-dispersive spectrometry (EDS, XMAX50). The X-ray photoelectron spectroscopy (XPS, ESCALABA 250XI)

measurement was applied to characterize the chemical valence state information of samples. The ultraviolet-visible (UV-vis) diffuse reflection spectroscopy (DRS) was tested by UV-vis 2550, and the functional groups (N-H) were examined by Fourier transform infrared (FTIR, Nexus 470).

PEC-NITRR experiment

The PEC measurements were tested in an H-type electrolytic cell (Fig. S8), where samples, Ag/AgCl and Pt sheet were served as the working electrode, reference electrode and counter electrode, respectively. The cathode and anode compartments were filled with 0.5 M Na_2SO_4 solution (50 mL), and $NaNO_3$ (150 μg·mL^{-1} NO_3^-) was added into the cathode compartment as reactant. The working electrode was irradiated under 300 W xenon lamp (100 mW cm^{-2}). Linear-sweep-voltammetry (LSV) curves were performed at a scanning rate of 50 mV s^{-1}. Mott-Schottky data and photoelectrochemical impedance spectroscopy (PEIS) were measured by electrochemical instrumentation (Princeton, VersaSTAT3) in 0.5 M Na_2SO_4. In order to discharge the gas dissolved in electrolyte, Ar flow was continuously injected into cathode and anode compartments for 1 hour.

Analytical methods

Detection of NO_3^-: Firstly, 1.0 mL electrolyte was taken out and diluted to 10 mL. Then, 0.2 mL HCl (1 M) and 0.6 mL sulfamic acid solution (0.8 wt%) were added into the above solution. After 10 minutes, the absorbance was detected by UV-vis spectrophotometry at a wavelength range from 225 nm to 275 nm. The final absorbance of NO_3^- was calculated based on the following equation: $A = A_{225nm} - 2A_{275nm}$. The standard curve has been obtained through $NaNO_3$ solutions with different concentrations, and the corresponding absorbance ($Y = 0.0283x + 0.0193$) was shown in Fig. S9.

Detection of NO_2^-: The color reagent was configured as follows: 2.0 g p-aminobenzenesulfonamide was added to a solution composed of 25 mL water and 5.0 mL phosphoric acid, and then 0.1 g N-(1-naphthyl)-ethylenediamine dihydrochloride was dissolved in the above solution. The volume of solution was diluted to 50 mL. 20 mL PEC-NITRR reaction solution was taken out from the electrolytic cell, and added to the 0.8 mL color reagent. After standing for 20 minutes, the absorbance was tested by UV-vis spectrophotometry at a wavelength of 540 nm. The standard curve could be obtained through $NaNO_2$ solutions with different concentrations, and the corresponding absorbance ($Y = 0.7994x + 0.0109$) was shown in Fig. S10.

Detection of NH_3: The NH_3 yield was determined by Nessler reagent spectrophotometry. 15 mL PEC-NITRR reaction solution was taken out from the electrolytic cell, which then was mixed with 1.0 mL sodium potassium tartrate solution ($KNaC_4H_6O_6 \cdot 4H_2O$) and 1.0 mL Nessler's reagent. After standing for 10 minutes, the absorbance was tested by UV-vis spectrophotometry at a wavelength of 425 nm. The standard curve was linearly fitted by NH_4Cl solutions with different concentrations, and the corresponding absorbance ($Y = 0.1315x - 0.0007$) was shown in Fig. S11.

^{15}N isotope labeling experiment: To verify the source of N in NH_3, isotopic labeling experiments were carried out by using $Na^{15}NO_3$ (99%) as N-source. 50 mL $Na^{15}NO_3$ electrolyte solution (added 1.0 mL 0.05 M H_2SO_4) was concentrated to 5.0 mL, and the concentrated electrolyte was detected by ^{1}H nuclear magnetic resonance (NMR) (100 μL D_2O and 50 μL DMSO). Similarly, $^{14}NH_3$ was also qualitatively analyzed by this method, when $Na^{14}NO_3$ was used as the N-source.

Computational methods

The NH_3 yield rate (aq) was calculated by Eq. 1:

$$V_{NH_3} = (C_{NH_3} \times V) / (S \times t) \quad \text{(Eq. 1)}$$

The conversion of NO_3^- was calculated by Eq. 2:

$$NO_3^- \text{ conversion} = \Delta C_{NO_3^-} / C_0 \times 100\% \quad \text{(Eq. 2)}$$

The selectivity of the product calculated by Eq. 3-4:

$$NH_3 \text{ selectivity } (S_{NH_3}) = C_{NH_3} / \Delta C_{NO_3^-} \times 100\% \quad \text{(Eq. 3)}$$

$$NO_2^- \text{ selectivity } (S_{NO_2^-}) = C_{NO_2^-} / \Delta C_{NO_3^-} \times 100\% \quad \text{(Eq. 4)}$$

The Faradaic efficiency was defined from the electric charge consumed for synthesizing ammonia and total charge passed through the electrode according to Eq. 5:

$$\text{Faradaic efficiency} = (n \times F \times C \times V) / (M \times Q) \times 100\% \quad \text{(Eq. 5)}$$

C_0 is the initial concentration of NO_3^-. $\Delta C_{NO_3^-}$ is the concentration difference of NO_3^- before and after reaction. C_{NH_3} and $C_{NO_2^-}$ are the concentration of NH_3 and NO_2^- after reaction, respectively. V, S, and t stand for the electrolyte volume, the area of catalyst, and the PEC reaction time, respectively. n is the number of electrons transferred in the reaction, F is the Faradaic constant (96485 C mol^{-1}), C stands for the concentration of the product, V is the total volume of the reaction liquid, M is the molecular weight of the product, Q is the total charge passing the electrode.

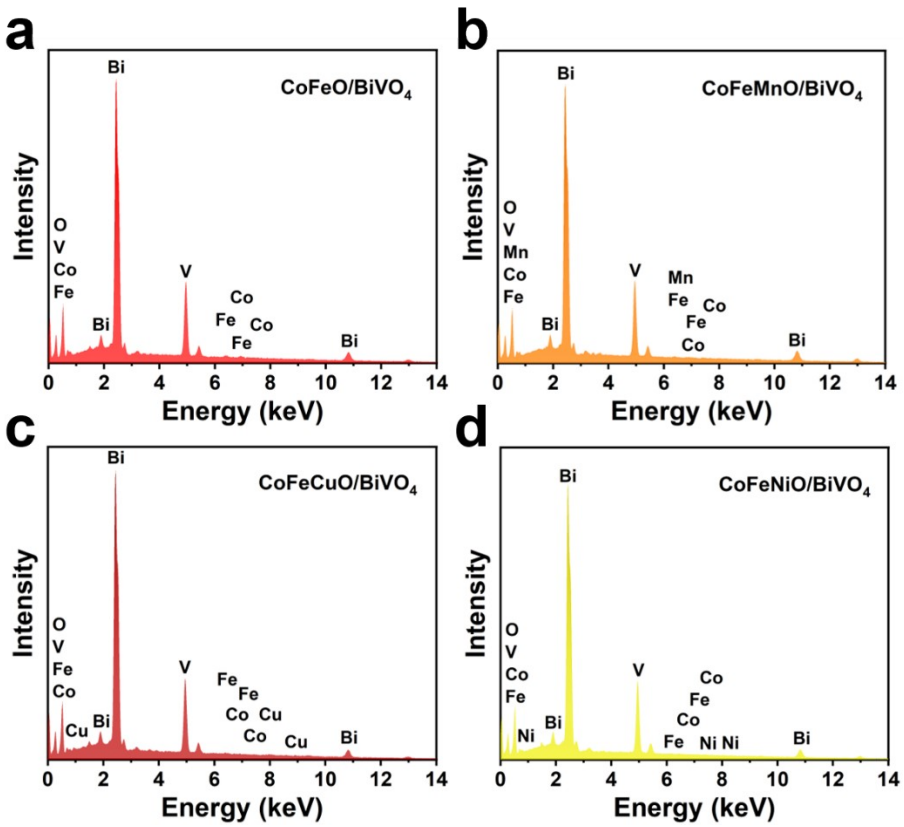

Fig. S1 The selective EDS spectra of (a) $CoFeO/BiVO_4$, (b) $CoFeMnO/BiVO_4$, (c) $CoFeCuO/BiVO_4$, (d) $CoFeNiO/BiVO_4$.

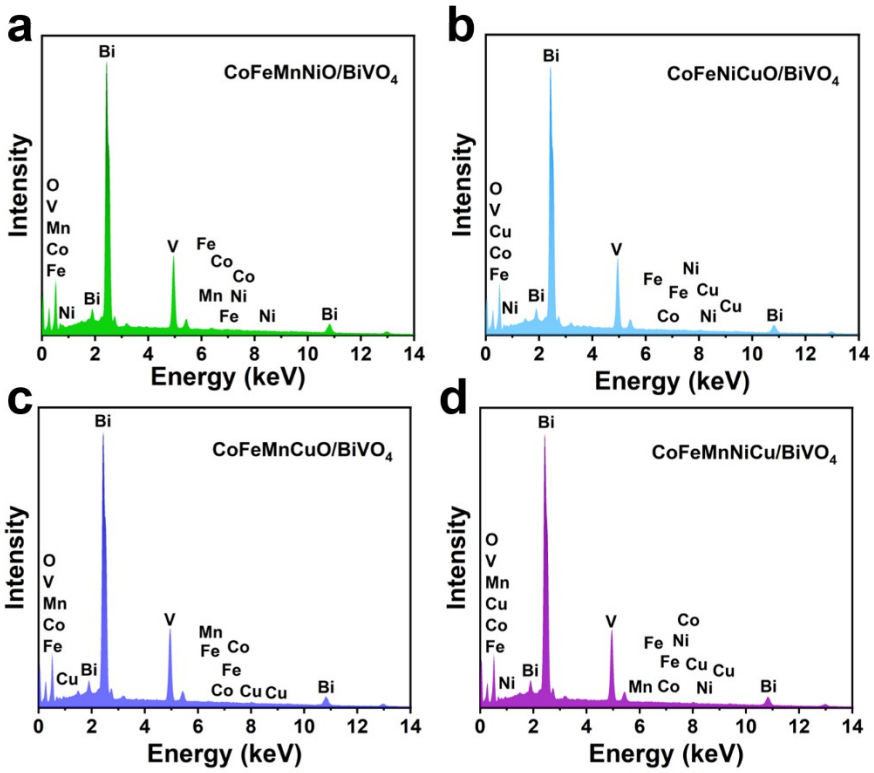

Fig. S2 The selective EDS spectra of (a) $CoFeMnNiO/BiVO_4$, (b) $CoFeNiCuO/BiVO_4$, (c) $CoFeMnCuO/BiVO_4$. (d) $CoFeMnNiCuO/BiVO_4$.

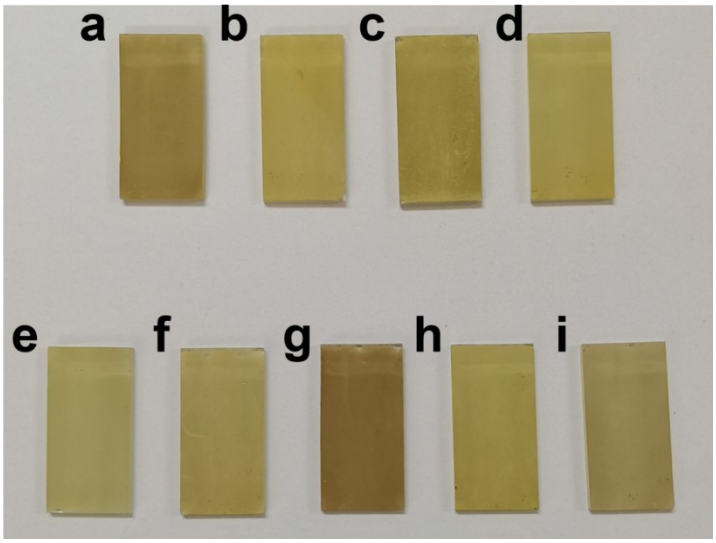

Fig. S3 Digital photos of (a) CoFeMnCuO/$BiVO_4$, (b) CoFeNiCuO/$BiVO_4$, (c) CoFeMnNiCuO/$BiVO_4$, (d) CoFeMnNiO/$BiVO_4$, (e) p-$BiVO_4$, (f) CoFeO/$BiVO_4$, (g) CoFeCuO/$BiVO_4$, (h) CoFeNiO/$BiVO_4$, (i) CoFeMnO/$BiVO_4$.

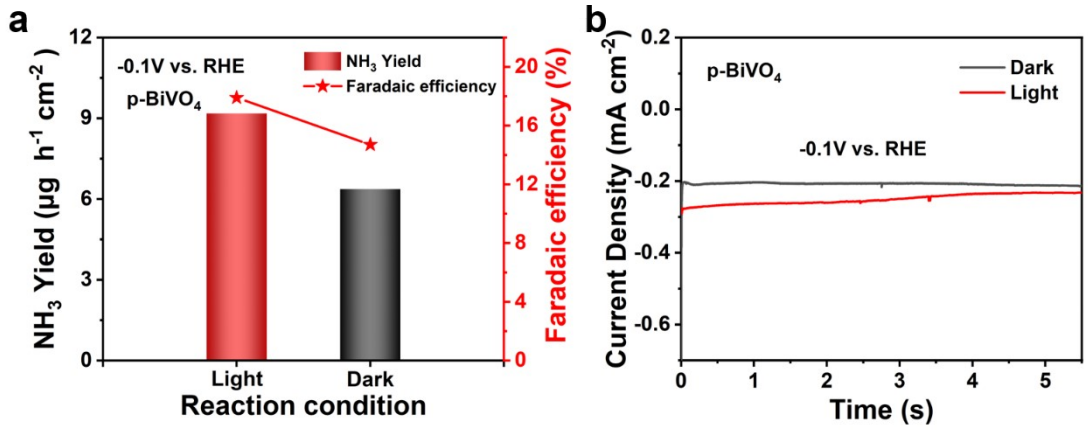

Fig. S4 (a) The p-$BiVO_4$ NH_3 yield and Faradic efficiency under light/dark conditions. (b) Stability of p-$BiVO_4$ under light/dark conditions.

Table S1 R_{ct} values of $CoFeMnO/BiVO_4$, $CoFeNiO/BiVO_4$, $CoFeCuO/BiVO_4$, $CoFeO/BiVO_4$, p-$BiVO_4$, $CoFeMnNiO/BiVO_4$, $CoFeMnNiCuO/BiVO_4$, $CoFeNiCuO/BiVO_4$ and $CoFeMnCuO/BiVO_4$.

Samples	R_S ($\Omega \cdot cm^2$)	R_{ct} ($\Omega \cdot cm^2$)
$CoFeMnO/BiVO_4$	1395	1166
$CoFeNiO/BiVO_4$	1630	1780
$CoFeCuO/BiVO_4$	1945	2246
$CoFeO/BiVO_4$	2110	2671
p-$BiVO_4$	2167	2685
$CoFeMnNiO/BiVO_4$	2101	2884
$CoFeMnNiCuO/BiVO_4$	2182	2938
$CoFeNiCuO/BiVO_4$	2506	3362
$CoFeMnCuO/BiVO_4$	3666	3473

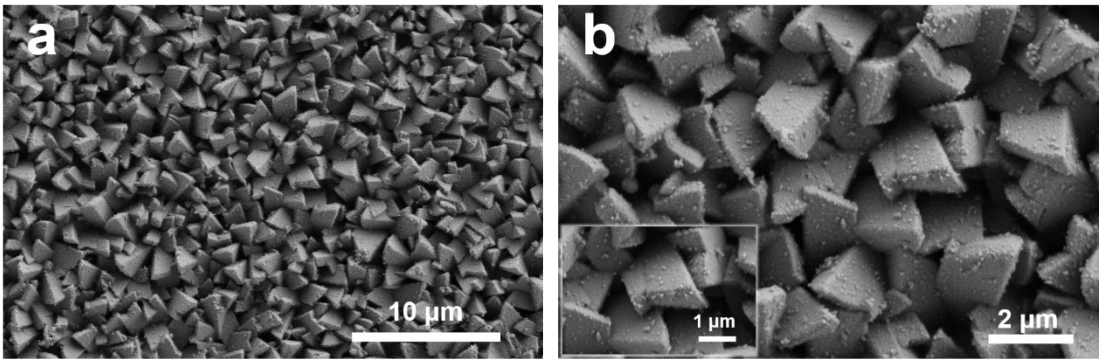

Fig. S5 (a) and (b) SEM images of CoFeMnO/$BiVO_4$ after stability test.

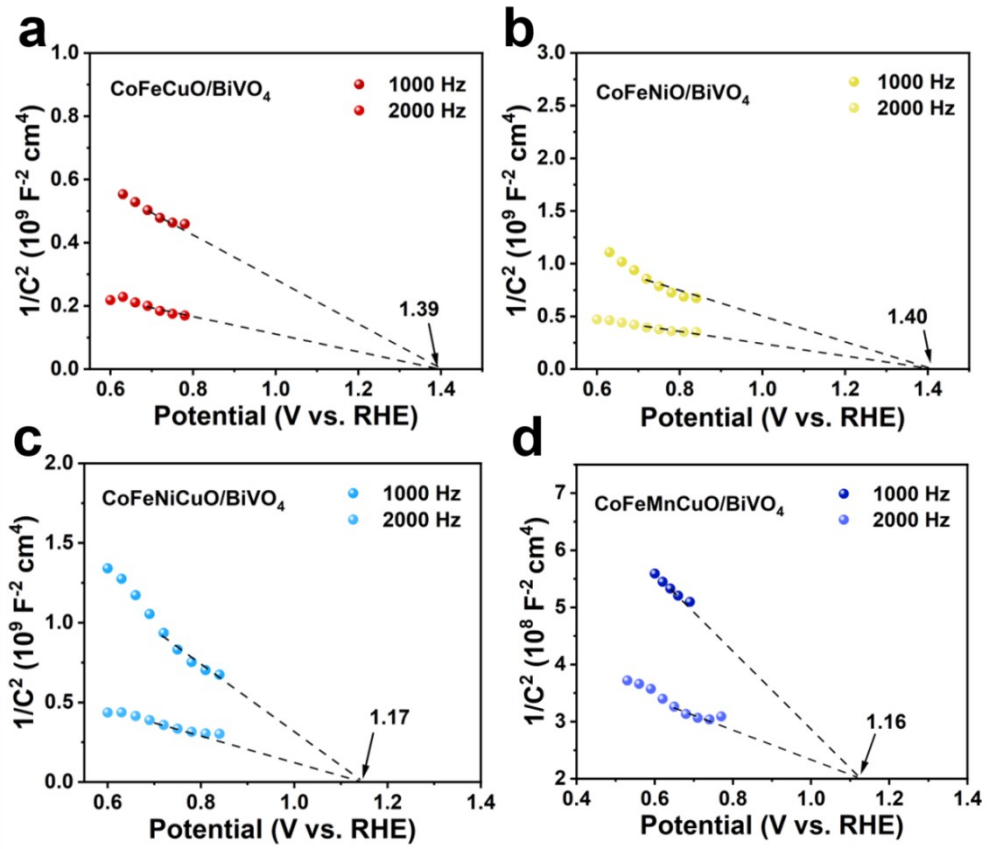

Fig. S6 Mott-Schottky plots at 1000Hz and 2000Hz: (a) $CoFeCuO/BiVO_4$, (b) $CoFeNiO/BiVO_4$, (c) $CoFeNiCuO/BiVO_4$, (d) $CoFeMnCuO/BiVO_4$.

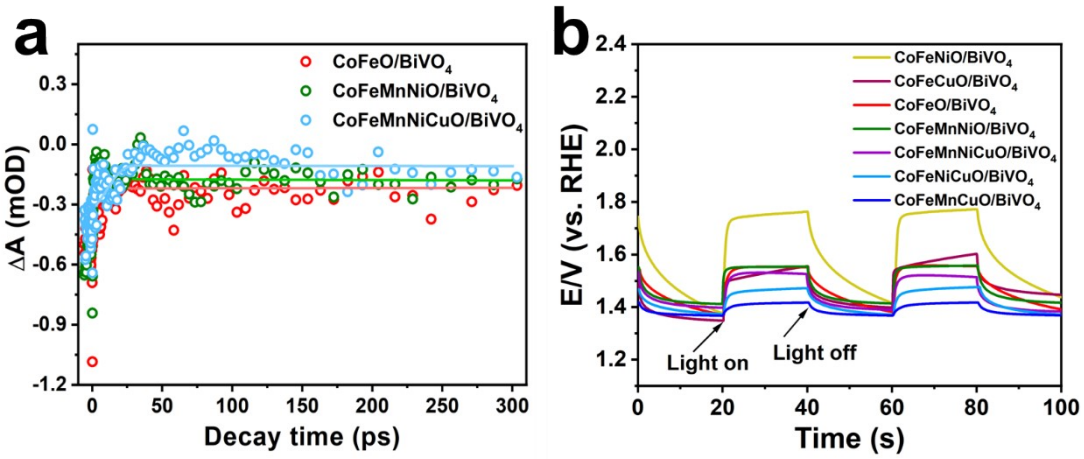

Fig. S7 (a) Characteristic dynamics for $CoFeO/BiVO_4$, $CoFeMnNiO/BiVO_4$ and $CoFeMnNiCuO/BiVO_4$ probed at 480 nm. (b) OCP of $CoFeNiO/BiVO_4$, $CoFeCuO/BiVO_4$, $CoFeO/BiVO_4$, $CoFeMnNiO/BiVO_4$, $CoFeMnNiCuO/BiVO_4$, $CoFeNiCuO/BiVO_4$ and $CoFeMnCuO/BiVO_4$ samples.

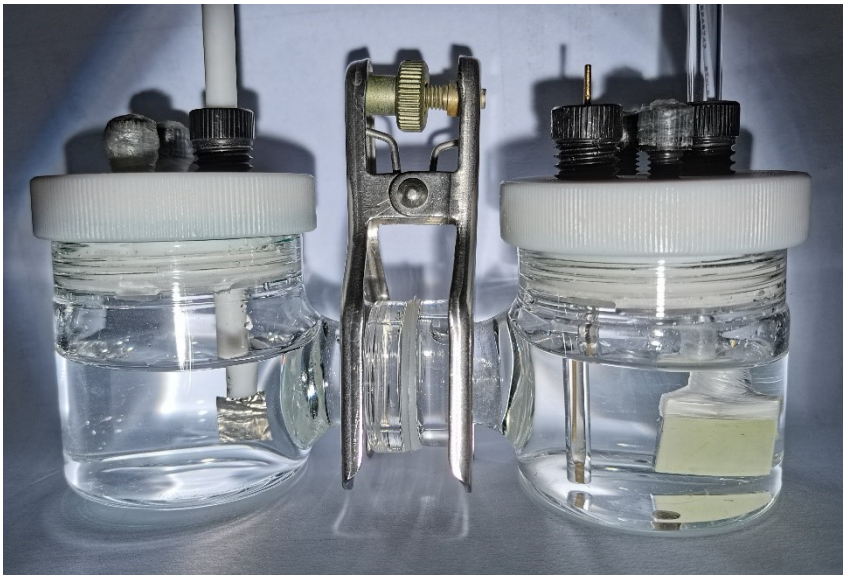

Fig. S8 Configuration of PEC-NITRR cell.

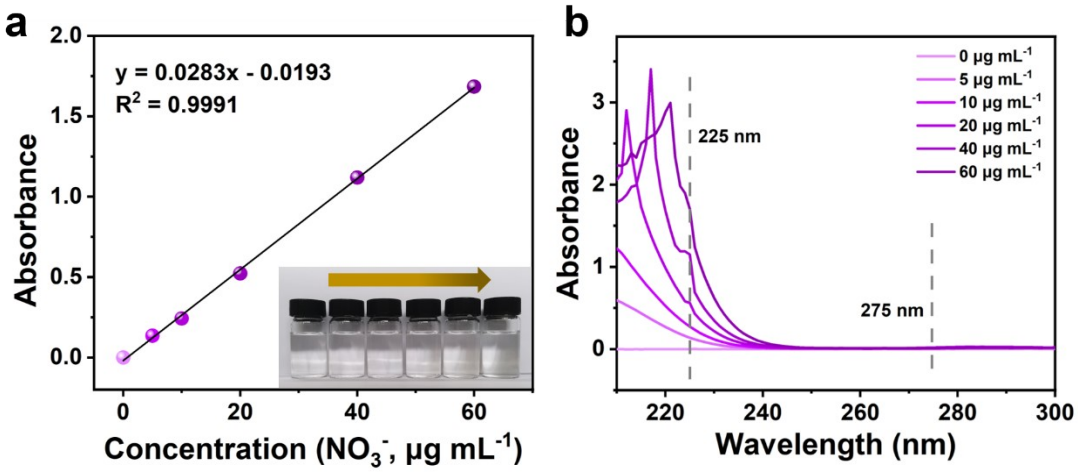

Fig. S9 (a) Standard curve of NO_3^- solutions with different concentrations and corresponding absorbance. (b) UV-vis absorption spectra.

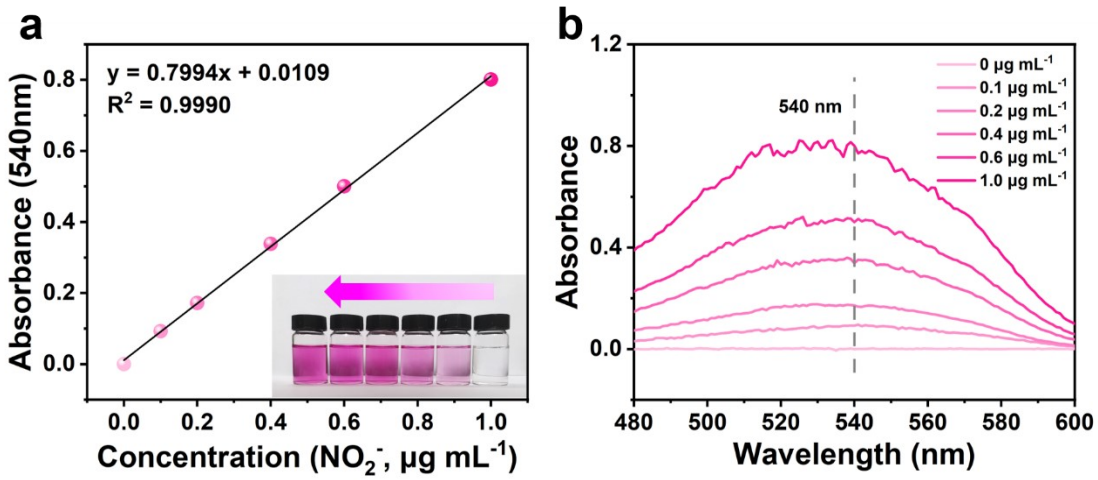

Fig. S10 (a) Standard curve of NO_2^- solutions with different concentrations and corresponding absorbance. (b) UV-vis absorption spectra.

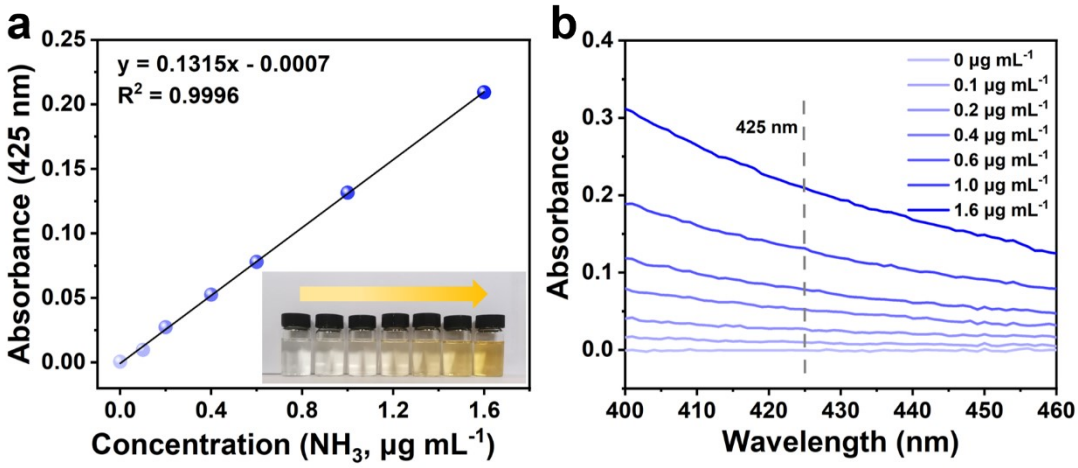

Fig. S11 (a) Standard absorbance curve for NH_3 yield by Nessler reagent spectrophotometry and (b) corresponding absorbance curve.

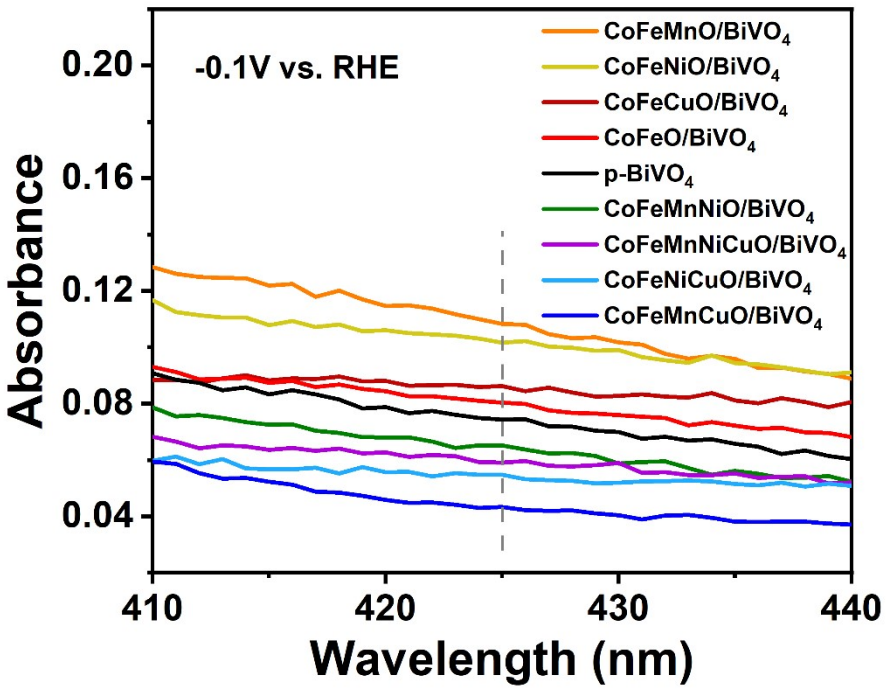

Fig. S12 UV-vis absorption curves and corresponding absorbance values at 425 nm of the 0.5 M Na_2SO_4 electrolyte.

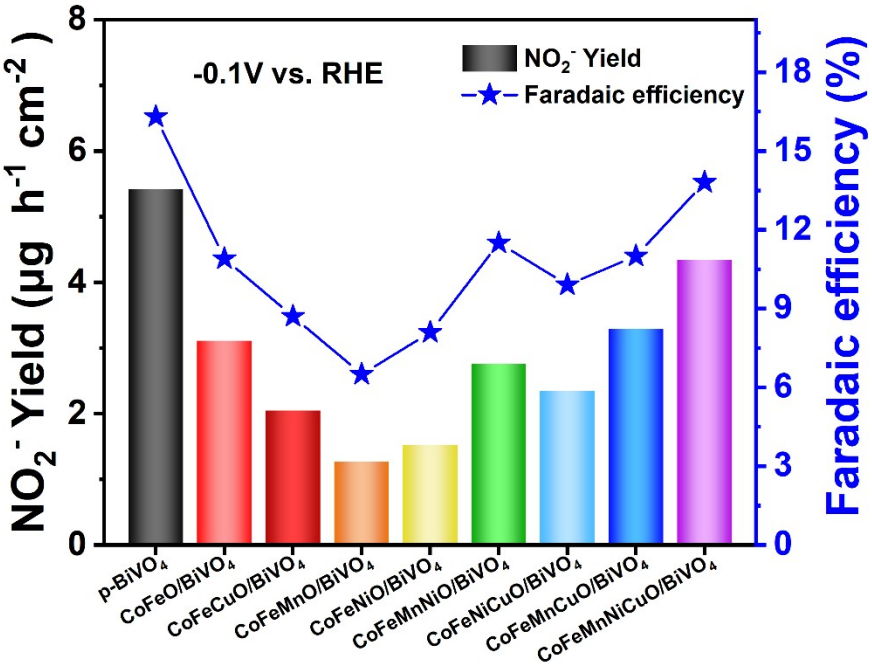

Fig. S13 The NO_2^- yield and Faradic efficiency of samples.

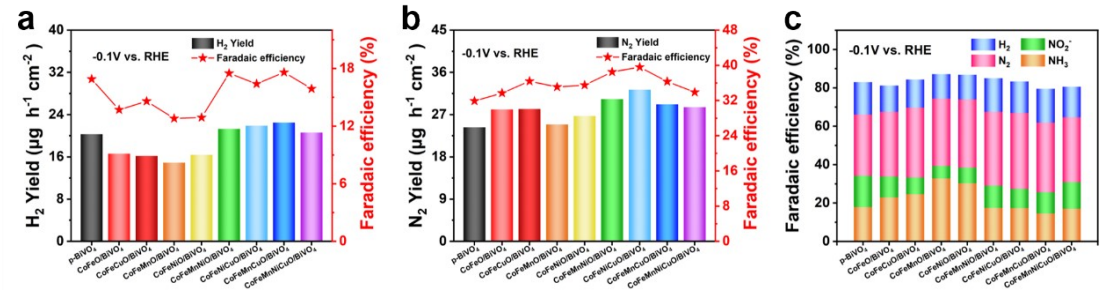

Fig. S14 Yield and Faradic efficiency of (a) H_2, (b) N_2. (c) Total Faradic efficiency in A-M_xO_y/$BiVO_4$.

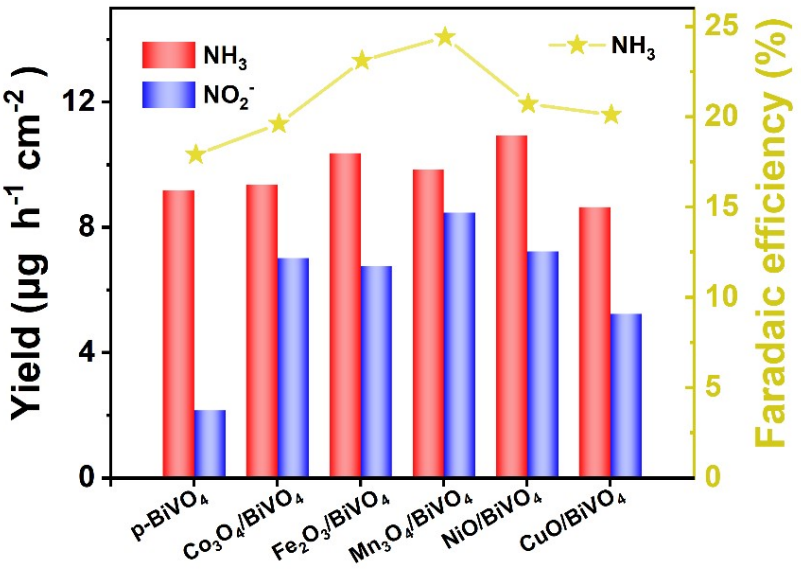

Fig. S15 Yield and Faradic efficiency of A-M_xO_y/p-$BiVO_4$ (M = Co, Fe, Mn, Ni, Cu) at -0.1 V vs. RHE.

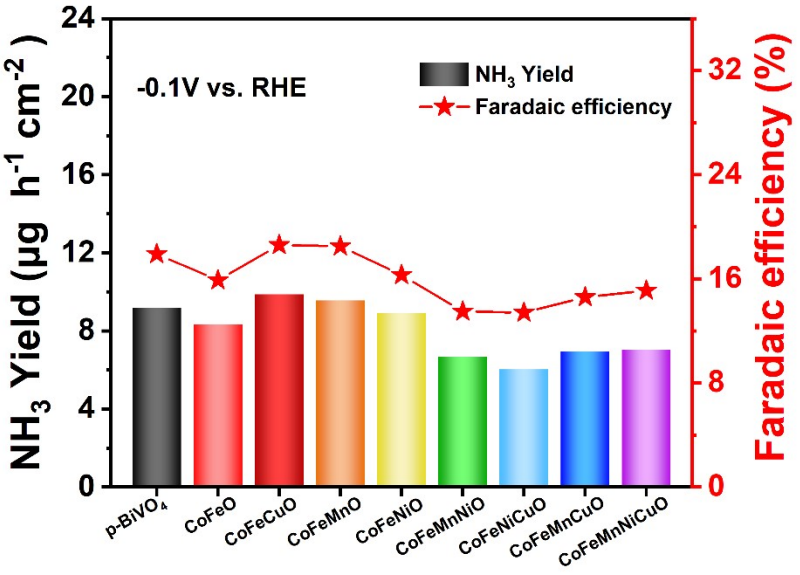

Fig S16 Yield of NH_3 and Faradic efficiency of A-M_xO_y at -0.1 V vs. RHE.

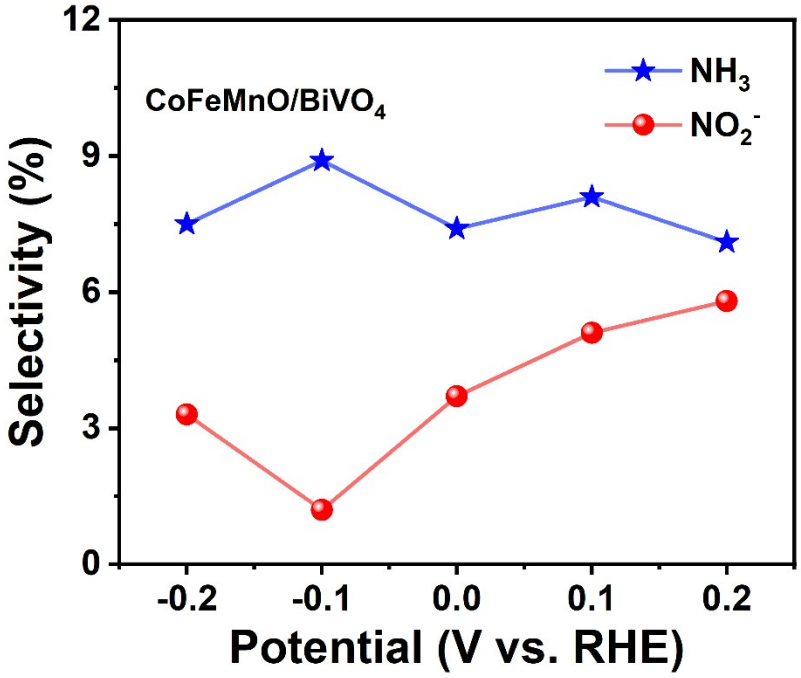

Fig. S17 Selectivity of $CoFeMnO/BiVO_4$ at different voltages.

Table S2 A specific mass ratio of hybrid catalysts.

Samples / Mass (g) / Chemicals	a	b	c	d	e	f	g	h
$Co(OAc)_2 \cdot 4H_2O$	0.06	0.03	0.03	0.06	0.02	0.03	0.03	0.02
$FeCl_2 \cdot 2H_2O$	0.03	0.03	0.03	0.015	0.03	0.015	0.015	0.015
$Mn(OAc)_2 \cdot 4H_2O$		0.03			0.02	0.03		0.02
$Ni(OAc)_2 \cdot 4H_2O$			0.03		0.02		0.03	0.02
$CuCl_2 \cdot 2H_2O$				0.015		0.015	0.015	0.015

Samples: (a) $CoFeO/BiVO_4$, (b) $CoFeMnO/BiVO_4$, (c) $CoFeNiO/BiVO_4$, (d) $CoFeCuO/BiVO_4$, (e) $CoFeMnNiO/BiVO_4$, (f) $CoFeMnCuO/BiVO_4$, (g) $CoFeNiCuO/BiVO_4$, (h) $CoFeMnNiCuO/BiVO_4$.